WWW.IJRPR.COM

International Journal of Research Publication and Reviews

Journal homepage: www.ijrpr.com ISSN 2582-7421

Image Denoising for Effective Fake Image Identification using CNN

L Praveen Kumar[1], G Anil Kumar[2]

[1,2]Department of Electronics and Communication Engineering.Anurag University.

Abstract –

Noise and blur may be removed from a photograph during picture restoration. Erasing camera shaking, radar imaging, and the influence of an image system's reaction to blurry images is challenging in many instances, including photography. Unwanted signals such as thermal or electrical noise or precipitation or snow in a picture are examples of image noise. The deterioration of the picture might be caused by coding, resolution restriction, transmission noise, object motion, camera shaking, or a combination. A sensor, such as a thermal or electrical signal, or an ambient, such as snow or rain, might cause an image to be blurred. There are several probable causes of picture degradation, including coded pictures, resolution restrictions, transmission noise, object motion, camera shaking, and these factors. Distinguishing between high- and low-frequency components may be accomplished by a process known as "picture decomposition," which entails separating a distorted image into two distinct layers, one for texture and the other for structure , from the LF. The present approach is based on a deep CNN architecture that is very customizable and takes advantage of the frequency characteristics of different sorts of artifacts. The same technique may be used for a wide range of image restoration projects by just altering the architecture. Using a quality improvement network based on residual and recursive learning is recommended to reduce noises with similar frequency characteristics. In order to prevent the network from dying, the authors used residual learning to speed up the training process. The researchers also developed new auxiliary classifi ers. The surtax was applied to the outputs of two inception modules, and an auxiliary loss over the same labels was calculated, much as in the prior experiment. Weighted averages are used to calculate the total loss function. Recursive learning may drastically decrease the number of training parameters while maintaining or increasing performance, as seen below. It is claimed that the proposed system is built on a pure version of Inception that does not include any leftover connections. Memory optimization or backpropagation may train it without splitting the copies.

Keywords- CNN, CFF, CFFN, and Deep FD are examples of convolutional neural networks.

I. INTRODUCTION

In image restoration, noise is removed and blur when a picture is retrieved from its original location. Camera shake, radar imaging, and image system response to blur contribute to motion blur in certain situations, such as photography. In an image, picture noise is an unwanted signal that emerges due to a sensor, such as a thermal or electrical signal, or the environment, like rain or snow, distorting the image. Object motion and camera shaking are all potential implications of image degradation, as are coded images and resolution restrictions. Images may be broken down into two distinct layers: one for the texture and one for the structure. The purpose of image decomposition is to separate these two levels to be seen independently. A facial expression of any prominent politician produces serious issues in society, politics, and business. The requirement for an accurate way of spotting fake faces in photos is thus crucial. Since our earlier studies, we've developed an effective method for detecting and removing fake photographs.

There are two sorts of forensics systems often utilized in traditional photo forgery detection procedures: active and passive schemes. When an external signal (such as a watermark) is added to a picture as part of the watermarking process, no visual artifacts are introduced into the active algorithms. This approach is used to extract the watermark from the target image to determine whether the image has been tampered with. It is possible to utilize the watermark picture to identify changed areas in the target image.

Since there is no source image in the GAN-generated images, the active image forgery detection system cannot retrieve the watermark image in this circumstance. Photo forgery detectors that use statistical information about an image's original are passive. Thus, the statistical information in the picture may be utilized to identify faulty areas. Passive photo forgery detectors cannot detect gANs because they are constructed from a low- dimensional random vector. The GAN-generated fake photographs are, in reality, similar to the originals (fig.1)

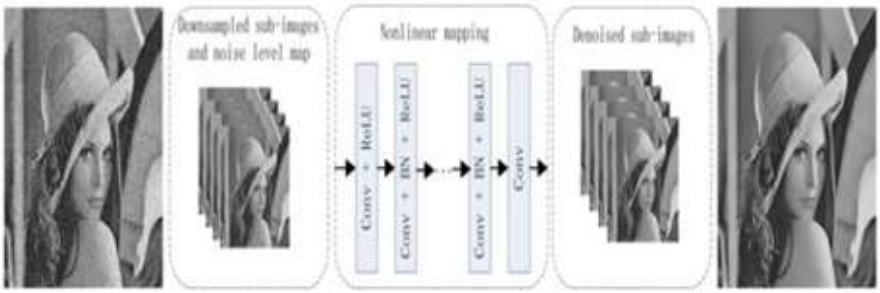

Fig. 1: Denoised Sub Images

II. RELATED WORKS

Disruption may cause visual information stored in pictures to be distorted by various factors. It is currently regarded as an essential part of any image processing process. Designed to reduce background noise and emphasize the image's distinctive features. Image denoising relies heavily on machine learning because of its scalability, accuracy, and speed. According to this research, a wide range of noises, such as the Gaussian and

Poisson noises and the mixed and real-world sounds, maybe denoised using cutting-edge machine-learning-based image de- nosiers such as convolutional neural networks and generative adversarial networks. Nosier's rationale, method, and framework for numerous machine learning algorithms were examined. 'There are several benchmark datasets in which various de-nosiers are compared, promising the findings.

Gaussian noise may be removed using GCBD, BRD Net, and de-nosier techniques. In reducing impulsive noise, both CNN+PSO and blind CNN function well. Several algorithms, such as WDL, EM-CNN, CNN, SDL, and Mixed CNN, may eliminate mixed noise. These two denoising methods, GRDN and DDFN, are accurate when applied to real-world data. This article presents the results of a study and evaluation of machine learning approaches for noise reduction. Three less-expensive types of models may be utilised today: dictionaries, CNNs, and GANs. a study of contrasts. PSNR results for different de noises' on a variety of benchmark datasets are offered to aid the reader. It has been proven that machine learning models may benefit from analytical approaches.

A. Drawbacks

- Inaccurate models lead to systems that under- or over- perform
- Heavyweight
- Cannot meet current network business demands
- This system is Opportunistic and uncontrollable
- The high complexity of installing and maintaining

B. Literature Review

New computer vision applications have increased the importance of picture de-noising. Noise corruption in digital photographs may be caused by various reasons, including camera sensors, lighting levels, A/D converter transmission, timing faults, storage sensor memory location problems, recording media, transmission channel interference, and compression artefacts. Low light and shorter exposure periods and longer exposure times impair the picture quality in biological imaging. Image restoration is necessary for medical imaging, remote sensing, underwater de-noising, and de- hazing. Medical imaging modalities, such as computed tomography (CT), magnetic resonance imaging (MRI), X-ray, and PET, use appropriate de-noising processes to provide patients with accurate diagnoses and treatment options. There is also a de-noising step in pre-processing before tackling the medical image classification or segmentation problem.

[1]. Synthetic aperture radar image de-noising may be done using a novel strategy that incorporates LPG, PCA, and a guided filter, among other approaches. In this scenario, there is a two-step method. In the beginning, we used coarse filters to reduce noise and eliminate speckles from the picture. Part two of the operation has now been completed. After transforming the original SAR image to the additive noise model with deviation correction, the SAR image is returned to the original SAR model. The pixel and its closest neighbors are then used as a vector based on a block similar matching to Using LPG, choose training samples from the local window. Because of this, you can be guaranteed that only similar sample patches will be utilised in the local statistical computation of the PCA transform estimate, allowing you to learn more about the image's local features by employing LPG. During the second phase, we apply guided filtering to effectively remove minor artifacts left behind by coarse filtering in the first stage of the PCA domain reduction process. Based on experimental data from both simulated and actual SAR pictures, the suggested technique surpasses current methods for image denoising in terms of a peak SNR, a structural similarity index, and an equal number of glances, all included in this analysis. Drawbacks: Narrowly focused expertise. This is a system that is uncontrolled and opportunistic. Due to the subjective nature of human vision, the annotations are inaccurate.

[2]. As a kind of spectrum imaging in photon-counting CT, we study principal component analysis (PCA) feasibility. Methods: Using data collected by a prototype system and computer simulations, we examine the possibilities of spectrum imaging in photon-counting CT using PCA for feature extraction and the implications of data standardization and de-noising on its performance. For tomographic image reconstruction, PCA in the projection domain maintains data consistency and is almost equivalent to PCA in the image domain. The first three fundamental components account for more than 99.99% of the data covariance. The first principal component picture may have a higher contrast-to-noise ratio (CNR) than the second component image. For even greater significance, the CNR for images made using data from all energy bins is likely higher than for images created using just the first main component (i.e., the conventional polychromatic CT image). Furthermore, de-noising decreases image noise and increases PCA's ability to extract features. Spectral imaging using PCA in photon- counting CT may be performed either in the projection or image domains. CT as a spectrum imaging technique and PCA's potential advantage in CNR over classic polychromatic CT has theoretical and practical significance.

Drawbacks: Computer-intensive and necessitating a considerable amount of RAM. and a lot of muscle. Installation and maintenance are quite difficult.

[3]. Wavelet-domain satellite image denoising should be optimized using the recently announced Multi-population differential evolution aided Harris Hawks Optimization Algorithm (CMDHHO). Unlike the HHO algorithm, this incorporates chaotic, multi-population, and differential evolution techniques. Noise suppression using CMDHHO- based noise suppression and Threshold Neural Network (TNN) methodologies were evaluated in this study, which examined a range of optimization strategies. The CMDHHO strategy has yielded superior qualitative and quantitative results compared to previous optimized and TNN-based noise reduction strategies. Additional advantages of this method include improved quality and quantity and a reduction in computing effort.

It takes a long time to refresh the messages. There hasn't been a full inquiry. In the case of large datasets, the difficulty of making accurate predictions is much greater.

[4]. With the recent increase in undersea activity, high- resolution sonar sensors placed on autonomous vehicles have been created. These vehicles are employed to find lost ships, archaeological artifacts, or even hidden mines under the waves. Highlights and shadows are important to differentiate from the object's background, shown in the seafloor backdrop. The segmentation of sonar images is used to achieve this. The automated segmentation of sonar images is the subject of this research. An improved fuzzy-based Kernel metric approach for sonar image segmentation is presented in this study, which incorporates two new fuzzy terms for local spatial and statistical information. When paired with the original image and a preliminary denoising algorithm, our method generates a segmentation strategy adapted to the inhomogeneity and complicated bottom texture of sonar data. We could verify the accuracy of our method by employing a combination of computer simulations, real-world sonar data, and data from two separate sea studies, including both multi-beam and synthetic aperture sonar. There are several drawbacks, such as the lengthy process. The cost of training a model is high. Opportunistic and reckless actors populate this system.

[5]. A previously unpublished method of photographing complicated motion objects with a low signal-to-noise ratio using bistatic inverse synthetic aperture radar (ISAR) (SNR). Its non-mirror-reflecting shape is blamed for the bistatic ISAR system's worse signal-to-noise ratio (SNR) than the monostatic ISAR system. Improved de-noising techniques for range profiles have been reported [6]. In order to create a noise reduction window, the approach non-coherently aggregates the matched range profiles. So that ISAR pictures may be properly focused, a CPI selection technique is presented in order to discover an interval where the Doppler is generally steady in order to create well-focused ISAR images as a consequence of complicated target motion [7-11]. An instantaneous Doppler spectrum with high resolution must be obtained using the reallocated time-frequency approach, and the lowest entropy criterion must be used to pick the best CPI. Furthermore, the CPI often lacks the pulses needed to produce high-resolution ISAR images [12]. The Laplacian scale mixture (LSM) model serves as the sparse prior for an ISAR imaging approach based on sparse apertures that functions in the Bayesian framework [13]. The Laplacian scale mixture (LSM) model may be used to rebuild high-resolution ISAR pictures with low sidelobes from limited data [14-19]. As far as resolution and noise reduction goes, the suggested LSM-based ISAR imaging strategy has been shown to beat the classic sparse Bayesian learning method [20]. The suggested algorithms' efficacy has been shown experimentally using simulated and measured data [22-25]. Model training requires many computing resources, which has several drawbacks. Order Understanding the link between components is not feasible. Inaccurate models lead to systems that under or over-perform [26].

C. Proposed System

Low-resolution pictures are often up-sampled using interpolation in the recommended method, and then nonlinear networks are utilized to obtain ultra-high resolution outputs. Due to high-resolution pictures in-network reasoning, these approaches incur a significant performance penalty. Alternatively, the image's nonlinear mapping may be computed on a low-resolution scale before being up-sampled via DE convolution, pixel shuffle, or other approaches. Inception is the single source of inspiration for this system, and no other influences have been considered [27-31]. Using memory optimization and backpropagation, it is feasible to train it without dividing the replicas [32]. The authors implemented two auxiliary classifiers to prevent the network's middle component from dying [33-36]. Under consideration is the system. Among the nonlinear components employed in picture restoration are skip connections of various densities, batch normalization, gate units, and other features.

D. Prejudicial Characteristic Training

An issue with supervised learning is the difficulty determining which topics were not covered throughout the training period. We use the contrastive loss to train the CFFs through paired learning, which improves the proposed strategy's performance. In order to accept paired inputs, the Siamese network architecture is used, as shown.

It might be difficult to determine which students are missing out on the instruction when using supervised learning. We apply the contrastive loss to train the CFFs through paired learning to enhance the proposed method's performance. Because of this, the Siamese network topology is employed to accept paired inputs, as shown fig. 2.

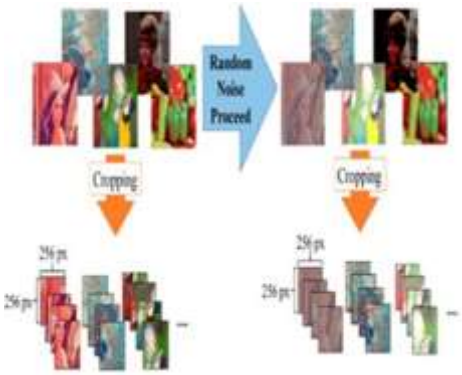

Fig. 2: Generating target and input patches

E. Learning Discriminative Characteristics

An issue with supervised learning is the difficulty determining which topics were not covered throughout the training period. We use the contrastive loss to train the CFFs through paired learning, which improves the proposed strategy's performance. In order to accept paired inputs, the Siamese network architecture is used, as shown.

It might be difficult to determine which students are missing out on the instruction when using supervised learning. We apply the contrastive loss to train the CFFs through paired learning to enhance the proposed method's performance.

Because of this, the Siamese network topology is employed to accept paired inputs, as shown.

F. Fake Image Recognition

False general image detection is more difficult than false face image detection because the content of a general picture varies widely. A general image's fake feature is more sophisticated than a face image's false feature. A more effective backbone network is needed to capture the CFFs of a generic picture, as contrasted to the backbone network used for identifying phony faces. The projected CFFN will have more channels as a result of this.

There is an increase in the density of blocks in each dense unit. The number of channels in each dense block is also increased in order to better capture overall image deceptive features. In order to determine whether or not an image is genuine, an equivalent sub-network to the contrastive loss and classification sub-network discussed in Section II is used.

G. Data Collection

Realistic visuals with high resolution could not be synthesized before the PGGAN. There were only 6464 pixels in the created face pictures using the public source code. Many artifacts would be seen if the false image's dimensions were adjusted to 128128 pixels, making it easier to distinguish it from the real one. In this case, there would be no need for a fake picture detector. Fewer than 64 64 pixels might be used to create convincing fake pictures by most GANs. Using 64 64 pixels as the input picture size. The best GAN model available at the time was used in the PGGAN. Nevertheless, the PGGAN may produce high-resolution fake face pictures, the size of which differs from that employed in our research. Consequently, we sampled the PGGAN-generated fake face picture to 64 64 throughout our research.

Note that the produced images obtained from the authors' PGGAN-provided official website.

III. SYSTEM ARCHITECTURE

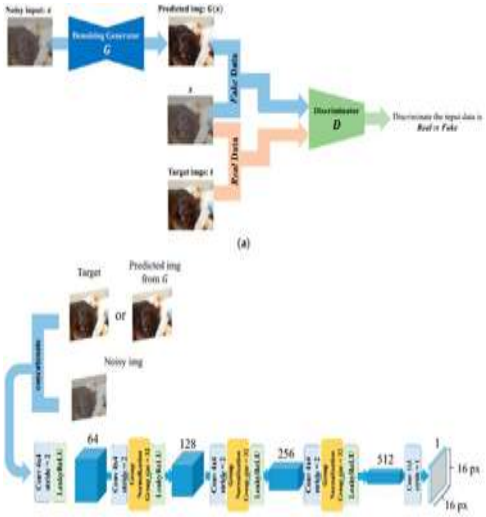

Fig. 3: Generates whether the input is real or fake, and it takes noisy pictures and outputs clean ones

The encoder has convolution layers, whereas the decoder has up-convolution (deconvolution) layers. In addition, the U-Net offers to skip connections between pathways. When the U-Net up samples feature maps, the preceding deconvolution layer's outputs are concatenated with the contracting path's feature maps (fig.3).

These findings prompted us to rebuild and deploy U-Net architecture as a generic denoising learner. We created three denoising models using the Group Normalization, Residual, and Dense U-Net Structure. We'll go through their construction and noise-reducing capabilities in the following sections.

A. Dataset Processing

The package is a complete progress bar package in Python that helps you develop scripts that update users on your application's progress. Supports Linux, Windows, Mac, FreeBSD, NetBSD, and Solaris/SunOS terminals and graphical user interfaces and I Python/Jupiter notebooks. A huge dataset, an expensive model to train, or a rapid evaluation of model performance call for a train-test split. A dataset is divided into two subsets. The model is first fitted to the training data. The second dataset is the test dataset. Data collection was fed into the machine learning algorithm during the training process. In this dataset, check how well the machine learning model fits. This experiment aims to evaluate the performance of a machine learning model using untrained data. The program ignores the data order by default. Real-world data preparation artefacts can be eliminated since the training and testing sets are generated randomly. Set the shuffle parameter to False to disable it (the default is true). The picture is read from the file using skimage.io.

B. Load Weights

Transfer learning is a very effective deep learning approach with many applications. Res Net and Inception, with their great performance and low computing cost, have been key to recent advances in image recognition. Using Inception-Res Net architecture with residual connections. Residual networks' neural network layers generate a graph, not a sequence. Parallel identity (repeater) shortcut links connect the first layer's input to the last layer's output. Each block has two parallel routes.

Like the previous networks, the left route uses sequential convolutional layers Plus batch normalization. The identity shortcut is on the correct route (also known as skip connection). An element-wise sum connects the two paths. An element from the first tensor is added to an element from the second tensor at the same place. Tensor output is the same as the input tensor. We distribute both the block's learned attributes and the original signal.

C. Prediction

These include 90-degree rotation, horizontal flipping, and vertical and horizontal shifting. The test set must be standardized. As part of the training, Image Data Generator creates augmented photographs. After max pooling, we'll create ELU activation functions for a single completely linked

layer. Padding=same is utilized. The output volume slices will be the same size as the input volume slices. Batch normalization enables you to handle data in the network's hidden layers like a standard score. So that the mean activation value is near zero and the standard deviation is near one, it normalizes the hidden layer outputs for each mini-batch. It works for convolutional and fully connected layers. Batch normalized networks may use higher learning rates.

IV. RESULTS AND DISCUSSIONS

The chainer deep-learning framework was used to implement denoise learning. In this case, the network was trained on two RTX 2080 Ti (11 GB) GPUs. Training each model took 90,067 training patches over 30 epochs using the Adam optimization function and a batch size of 5. Adam's hyperparameters were L1 norm loss, 0.001 learning rate, and 0.9 exponential momentum rate. We set the training parameters for the Generator and Discriminator to 0.0002 and 0.5, respectively, using L1 norm + adversarial loss (fig.4).

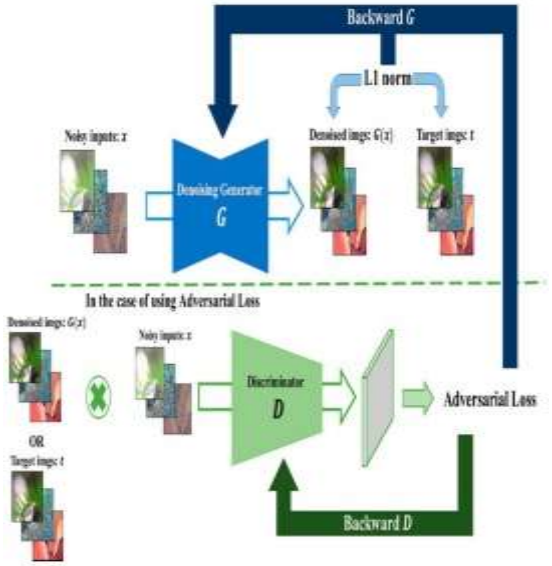

Fig. 4: Overview of the denoising training process

The Image Data Generator class enables data to be rotated 90 degrees, flipped, and moved horizontally and vertically. The test set has to be standardized. As part of the training, the Image Data Generator generates enhanced photographs. A single completely linked layer will be formed after the previous max pooling. Using the padding=same parameter. This implies that the output volume slices will match the input volume slices in size. Batch normalisation works like a regular score in the network's hidden layers. As a result, the mean activation value is near zero, while the standard deviation is close to one for each mini-batch (thus the name). For convolutional and fully connected layers. Batch normalised networks may learn at higher rates and train quicker.

A. Generating Patches from the Image

The input picture (the processed noisy image) was cropped to 256 256 patch sizes, and the target image was cropped to this size as well (the image before processing). Detailed instructions on how to make these patches may be found here. Our training set yielded a total of 20,120 photographs from which we were able to extract 90,067 patches. The deep denoising model uses the input patches rather than using the target patches as trained data.[21] the saved data can be used to find any malicious interpreted image's on websites using the RNN model and eliminates digital crimes.

V. CONCLUSIONS

Pairing learning with fake feature networks recognises the false face and general pictures of modern GANs. The proposed CFFN can train middle and high-level discriminative fake features by aggregating cross-layer feature layers (CLFR). Fake feature learning might be enabled in the proposed paired learning technique, allowing trained fake image detectors to recognise fresh GAN-generated false images even if they were not included in the training phase. Compared to existing state- of-the-art methodologies, the suggested strategy was demonstrated to be better in terms of accuracy and recall rate. We'll add object detection and a Siamese network structure to our recommended solution to combat misleading video detection.

References

[1] Kaur, P., Singh, G., & Kaur, P. (2018). A review of denoising medical images using machine learning approaches. Current medical imaging, 14(5), 675-685.

[2] Wang, E., & Nealon, J. (2019). Applying machine learning to 3D seismic image denoising and enhancement. Interpretation, 7(3), SE131-SE139.

[3] Li, H. (2014). Deep learning for image denoising. International Journal of Signal Processing, Image Processing, and Pattern Recognition, 7(3), 171-180.

[4] Rajwade, A., Rangarajan, A., & Banerjee, A. (2012). Image denoising using the higher order singular value decomposition. IEEE Transactions on Pattern Analysis and Machine Intelligence, 35(4), 849-862.

[5] Yang, Q., Yan, P., Kalra, M. K., & Wang, G. (2017). CT image denoising with perceptive deep neural networks. arXiv preprint arXiv:1702.07019.

[6] Dey, B., Halder, S., Khalil, K., Lorusso, G., Severi, J., Leray, P., & Bayoumi, M. A. (2021, February). SEM image denoising with unsupervised machine learning for better defect inspection and metrology. In Metrology, Inspection, and Process Control for Semiconductor Manufacturing XXXV (Vol. 11611, p. 1161115). International Society for Optics and Photonics.

[7] Liu, B., & Liu, J. (2019, March). Overview of image denoising based on deep learning. In Journal of Physics: Conference Series (Vol. 1176, No. 2, p. 022010). IOP Publishing.

[8] Liu, B., & Liu, J. (2019, March). Overview of image denoising based on deep learning. In Journal of Physics: Conference Series (Vol. 1176, No. 2, p. 022010). IOP Publishing.

[9] Gondara, L. (2016, December). Medical image denoising using convolutional denoising autoencoders. In 2016 IEEE 16th international conference on data mining workshops (ICDMW) (pp. 241-246). IEEE.

[10] Tassano, M., Delon, J., & Veit, T. (2019). An analysis and implementation of the FFDNet image denoising method. Image Processing On Line, 9, 1-25.

[11] Tassano, M., Delon, J., & Veit, T. (2019). An analysis and implementation of the FFDNet image denoising method. Image Processing On Line, 9, 1-25.

[12] Yang, X., Xu, Y., Quan, Y., & Ji, H. (2020). Image denoising via sequential ensemble learning. IEEE Transactions on Image Processing, 29, 5038-5049.

[13] Wang, G., Ye, J. C., Mueller, K., & Fessler, J. A. (2018). Image reconstruction is a new frontier of machine learning. IEEE transactions on medical imaging, 37(6), 1289-1296.

[14] Arshaghi, A., Ashourian, M., & Ghabeli, L. (2021). Denoising Medical Images Using Machine Learning, Deep Learning Approaches: A Survey. Current Medical Imaging, 17(5), 578-594.

[15] Li, Z., Baker, H., & Bajcsy, R. (2013, July). Joint image denoising using light-field data. In 2013 IEEE International Conference on Multimedia and Expo Workshops (ICMEW) (pp. 1-6). IEEE.

[16] Schuler, C. J., Christopher Burger, H., Harmeling, S., & Scholkopf, B. (2013). A machine learning approach for non-blind image deconvolution. In Proceedings of the IEEE conference on computer vision and pattern recognition (pp. 1067-1074).

[17] Wu, D., Kim, K., Fakhri, G. E., & Li, Q. (2017). A cascaded convolutional neural network for X-ray low-dose CT image denoising. arXiv preprint arXiv:1705.04267.

[18] Smets, B. (2019). Geometric image denoising and machine learning (Doctoral dissertation, Master's thesis, Eindhoven University of Technology)

[19] Dahlberg, H., Adler, D., & Newlin, J. (2019). Machine-learning denoising in feature film production. In ACM SIGGRAPH 2019 Talks (pp. 1-2).

[20] Honeine, P., & Richard, C. (2011). Preimage problem in kernel-based machine learning. IEEE Signal Processing Magazine, 28(2), 77-88.

[21] Aarthi, B., Jeenath Shafana, N., Flavia, J., Chelliah, B.J. (2022). A Hybrid Multiclass Classifier Approach for the Detection of Malicious Domain Names Using RNN Model. In: Smys, S., Tavares, JMRS, Balas, V.E. (eds) Computational Vision and Bio-Inspired Computing. Advances in Intelligent Systems and Computing, vol 1420. Springer

[22] Jain, A., Dwivedi, R. K., Alshazly, H., Kumar, A., Bourouis, S., & Kaur, M. Design and Simulation of Ring Network-on-Chip for Different Configured Nodes Computers, Materials, & Continua; Henderson Vol. 71, Iss. 2, (2022): 4085-4100.

[23] Kumar, A., & Jain, A. (2021). Image smog restoration using oblique gradient profile prior and energy minimization. Frontiers of Computer Science, 15(6), 1-7.

[24] Gupta, N., Vaisla, K. S., Jain, A., Kumar, A., & Kumar, R. (2021). Performance Analysis of AODV Routing for Wireless Sensor Network in FPGA Hardware. Computer Systems Science and Engineering, 39(2), 1- 12.

[25] Gupta, N., Jain, A., Vaisla, K. S., Kumar, A., & Kumar, R. (2021). Performance analysis of DSDV and OLSR wireless sensor network routing protocols using FPGA hardware and machine learning. Multimedia Tools and Applications, 80(14), 22301-22319.

[26] Misra, N. R., Kumar, S., & Jain, A. (2021, February). A Review on E- waste: Fostering the Need for Green Electronics. In 2021 International Conference on Computing, Communication, and Intelligent Systems (ICCCIS) (pp. 1032-1036). IEEE.

[27] Kumar, S., Jain, A., Kumar Agarwal, A., Rani, S., & Ghimire, A. (2021). Object-Based Image Retrieval Using the U-Net-Based Neural Network. Computational Intelligence and Neuroscience, 2021.

[28] Kumar, S., Jain, A., Shukla, A. P., Singh, S., Raja, R., Rani, S., ... & Masud, M. (2021). A Comparative Analysis of Machine Learning Algorithms for Detection of Organic and Nonorganic Cotton Diseases. Mathematical Problems in Engineering, 2021.

[29] Jain, A., & Kumar, A. (2021). Desmogging of still smoggy images using a novel channel prior. Journal of Ambient Intelligence and Humanized Computing, 12(1), 1161-1177.

[30] Ghai, D., Gianey, H. K., Jain, A., & Uppal, R. S. (2020). Quantum and dual-tree complex wavelet transform-based image watermarking. International Journal of Modern Physics B, 34(04), 2050009.

[31] Agrawal, N., Jain, A., & Agarwal, A. (2019). Simulation of Network on Chip for 3D Router Architecture. International Journal of Recent Technology and Engineering, 8, 58-62.

[32] Sharma, S. K., Jain, A., Gupta, K., Prasad, D., & Singh, V. (2019). An internal schematic view and simulation of major diagonal mesh network- on-chip. Journal of Computational and Theoretical Nanoscience, 16(10), 4412-4417.

[33] Agarwal, A. K., & Jain, A. (2019). Synthesis of 2D and 3D NoC mesh router architecture in HDL environment. Journal of Advanced Research in Dynamical and Control Systems, 11(4), 2573 -2581.

[34] Jain, A., Gahlot, A. K., Dwivedi, R., Kumar, A., & Sharma, S. K. (2018). Fat Tree NoC Design and Synthesis. In Intelligent Communication, Control and Devices (pp. 1749-1756). Springer, Singapore.

[35] Jain, A., Dwivedi, R., Kumar, A., & Sharma, S. (2017). Scalable design and synthesis of 3D mesh network on chip. In Proceeding of International Conference on Intelligent Communication, Control and Devices (pp. 661- 666). Springer, Singapore.

[36] Jain, A., Kumar, A., & Sharma, S. (2015). Comparative Design and Analysis of Mesh, Torus and Ring NoC. Procedia Computer Science, 48, 330-337.a